

Published in final edited form as:

Nat Struct Mol Biol. 2011 April ; 18(4): 500–503. doi:10.1038/nsmb.2029.

Homology-directed Fanconi anemia pathway crosslink repair is dependent on DNA replication

Koji Nakanishi¹, Francesca Cavallo², Loïc Perrouault³, Carine Giovannangeli³, Mary Ellen Moynahan⁴, Marco Barchi², Erika Brunet^{1,3}, and Maria Jasin^{1,*}

¹Developmental Biology Program, Memorial Sloan-Kettering Cancer Center, New York, NY, USA

²Department of Public Health and Cell Biology, Section of Anatomy, University of Rome Tor Vergata, Rome, Italy

³Muséum National d'Histoire Naturelle, CNRS UMR7196, and INSERM U565, Paris, France

⁴Department of Medicine, Memorial Sloan-Kettering Cancer Center, New York, NY, USA

Abstract

Homologous recombination (also termed homology-directed repair, HDR) is a major pathway for the repair of DNA interstrand crosslinks (ICLs) in mammalian cells. Cells from Fanconi anemia (FA) patients are characterized by extreme ICL sensitivity, but their reported defect in HDR is mild. Here, we examined ICL-induced HDR using a GFP reporter and observed a profound defect in ICL-induced HDR in FA cells, but only when the reporter could replicate.

FA is a rare recessive disease characterized by developmental abnormalities, bone marrow failure and cancer predisposition¹. Diagnosis of FA is based on increased levels of chromosome abnormalities after treatment of patient-derived cells with agents that cause ICLs¹. To date, FA patients have been found to have mutations in any of thirteen genes (*FANC* genes), the majority of which encode FA core complex members required for the monoubiquitylation of FANCI–FANCD2; the remaining *FANC* genes include the breast cancer susceptibility gene *BRCA2* (*FANCD1*) and genes that interact with BRCA1 and BRCA2². ICLs impede DNA replication, and recent studies with *Xenopus* cell free extracts have described replication fork dynamics at an ICL in molecular detail³. These studies have suggested that the monoubiquitylated FANCI–FANCD2 complex is required for incisions near the ICL and for translesion synthesis beyond the ICL⁴.

Although cell-free extracts have not been amenable to recapitulating HDR *in vitro*, cellular studies have demonstrated that mutation of either FA core complex members or the FANCD2 monoubiquitylation site results in HDR defects⁵. These defects, however, are mild compared with those resulting from BRCA2 deficiency⁶. In these previous studies, HDR was measured with the widely-used DR-GFP reporter where a DSB formed by I-SceI endonuclease results in GFP⁺ cells when repaired by HDR⁷ (Fig. 1a). Given the specific

*Corresponding author: Phone (212) 639-7438; FAX: (212) 772-8410; m-jasin@ski.mskcc.org.

AUTHOR CONTRIBUTIONS

K.N. designed and performed experiments, analyzed data, and assisted in manuscript preparation; F.C. performed experiments and analyzed data; L.P. prepared the ICL-only substrates; C.G. supervised L.P. and assisted in manuscript preparation; M.E.M. provide supervision, analyzed data, and assisted in manuscript preparation; M.B. supervised F.C. and contributed to data analysis; E.B. designed experiments and assisted in manuscript preparation; M.J. designed the experiments, supervised the project, and wrote the manuscript.

Competing interests

The authors declare no competing financial interests.

sensitivity of FA cells to agents that cause ICLs, we sought to address whether the FA pathway has a specific defect in HDR of ICLs. To test this, DR-GFP was modified to TR-GFP, which contains a specific site for ICL formation which is achieved using a triplex-forming oligonucleotide conjugated to psoralen (pso-TFO) (Fig. 1a,b and Supplementary Fig. 1a). This technology has previously been used to enhance recombination at specific sequences⁸⁻¹⁰. The pso-TFO:TR-GFP triplex was formed and then transfected into human U2OS cells; 1 hr post-transfection, cells were exposed to low dose UVA (0.15 J m^{-2}) to create the ICL^{11,12} (Supplementary Fig. 1c). ICL formation was verified by resistance of the ICL site in TR-GFP to DraI¹¹ (Fig. 1c and Supplementary Fig. 1d). After 48 hr, GFP⁺ cells were quantified by flow cytometry and found to be substantially induced by the ICL (Fig. 1d). In the absence of UVA or with TFOs which could not form an ICL in TR-GFP (*i.e.*, pso-mTFO, which is incapable of forming a triplex with TR-GFP, or an unconjugated TFO, which is inactive in HDR^{13,14}; $p=0.0003$), the percentage of GFP⁺ cells was significantly lower. These results confirm that HDR is induced specifically by the ICL and not by UVA or the TFO itself, and that no additional damage is required for HDR induction¹⁵.

To determine whether ICL-induced HDR requires canonical HDR factors, we tested the involvement of BRCA2⁶. We used V-C8 hamster cells which, like other BRCA2-deficient cells, are sensitive to both ICL and DSB-inducing agents¹⁶. We found that, relative to BRCA2-complemented cells, V-C8 cells had substantially reduced ICL-induced HDR as it did with DSB-induced HDR¹⁷ ($p<0.0001$; Fig. 1e).

We further tested mouse embryonic stem (ES) cell lines deficient in different DNA repair pathways. As reported previously and as demonstrated here, BRCA1 is required for efficient DSB-induced HDR⁶ (Fig. 2a and Supplementary Table 1). With the TR-GFP assay, we found that *Brca1*^{-/-} cells were also defective in ICL-induced HDR. These results implicate BRCA1 in playing an important role in repairing multiple types of lesions by HDR, like BRCA2, while further supporting the importance of HDR for ICL repair.

During DSB repair, HDR competes with nonhomologous end-joining (NHEJ) for access to DNA ends^{18,19}. A central component of the canonical NHEJ pathway, Ku70–Ku80, is thought to suppress HDR by blocking DNA end resection¹⁸. The DR-GFP plasmid assay used here recapitulates this suppression, as *Ku70*^{-/-} cells had higher levels of HDR than Ku70-complemented cells (Fig. 2b and Supplementary Table 1). While sensitive to agents that cause DSBs, *Ku70*^{-/-} cells have little or no sensitivity to ICL agents (Supplementary Fig. 2), indicating a specific role for NHEJ components in DSB repair. Consistent with this, we found that *Ku70*^{-/-} cells had similar levels of ICL-induced HDR as complemented *Ku70*^{-/-} cells (Fig. 2b). These results indicate that the ICL is not simply being converted to a DSB and that the TR-GFP assay provides a specific measure of ICL-induced HDR. As DNA ends are formed after incision next to an ICL (see below), FA pathway components or other proteins may possibly shield these intermediates from NHEJ proteins, as has been suggested by recent studies^{20,21}.

ERCC1-XPF is a structure-specific endonuclease involved in nucleotide excision repair, but it is also implicated in ICL repair, presumably by cleaving a structural intermediate²². *Ercc1*^{-/-} ES cells have little or no defect in DSB-induced HDR²³ (Fig. 2c and Supplementary Table 1). By contrast, these cells showed a reduced level of ICL-induced HDR compared with ERCC1-complemented cells, implicating ERCC1 specifically in the repair of ICLs.

These results with repair-deficient cells provide a framework with which to compare FA-deficient cells. FANCA is one of the FA core complex proteins which are crucial for FANCD2 monoubiquitylation²⁴. Like FA patient-derived cells, *Fanca*^{-/-} ES cells have a

small defect in DSB-induced HDR as assayed with either an integrated or plasmid DR-GFP reporter⁵ (Fig. 2d and Supplementary Table 1). Notably, we observed a similarly mild reduction in ICL-induced HDR.

Given the extreme sensitivity of FA cells to ICLs, it was surprising that a more profound defect in ICL-induced HDR was not apparent with FA pathway defects. As ICLs are well characterized as impediments to DNA replication³, we asked whether ICL-induced HDR can be coupled to replication. To test this, the TR-GFP reporter was modified to contain the origin of replication (OriP) from Epstein-Barr Virus (EBV), allowing it to replicate in human cells in the presence of the EBV nuclear antigen EBNA1²⁵ (TR-OriP-GFP; Fig. 3a and Supplementary Fig. 3a). For comparison, the DSB reporter was similarly modified (DR-OriP-GFP; Fig. 3a).

We tested the TR-OriP-GFP reporter in U2OS cells expressing EBNA1. GFP⁺ cells were obtained at a substantially higher frequency in cells expressing EBNA1 compared with cells not expressing EBNA1 ($p < 0.0001$; Fig. 3c). To rule out non-specific effects of EBNA1, we also compared TR-OriP-GFP with TR-GFP in cells expressing EBNA1. GFP⁺ cells were obtained at a substantially higher frequency with an ICL in TR-OriP-GFP than in TR-GFP ($p = 0.0002$; Supplementary Fig. 3b). Thus, both components – the replication origin and the origin binding protein – are required for the large induction of GFP⁺ cells after ICL formation. By contrast, DSB formation in DR-OriP-GFP resulted in only a small increase in GFP⁺ cells in the presence of EBNA1 ($p = 0.0002$; Fig. 3b). These results indicate that ICL-induced HDR is much more efficient when coupled to replication, whereas replication has little effect on DSB-induced HDR.

To address the role of the FA pathway in ICL-induced HDR coupled to replication, we examined FA patient-derived cells (GM6914) deficient in the core complex protein FANCA. In the absence of FANCA, ICL-induced HDR was low, whether or not EBNA1 was present (Fig. 3g). By contrast, in the presence of FANCA, ICL-induced HDR was substantially higher when EBNA1 was present ($p < 0.0001$; Fig. 3g). FANCA did not affect replication *per se*, as transfection of an OriP vector containing an intact *GFP* gene led to a similar increase in GFP⁺ cells with or without FANCA (Supplementary Fig. 3c).

The ICL in these previous experiments was formed in cells, but we also formed the ICL *in vitro* by directly treating pso-TFO:TR-OriP-GFP DNA with UVA (Supplementary Figs. 1c, 3d); ICL formation *in vitro* prior to transfection also induced HDR in a replication and FANCA-dependent manner ($p < 0.0001$; Figs. 3d,3h). DSB-induced HDR was also higher in the presence of FANCA, but the increase was small compared with ICL-induced HDR and was similar whether or not EBNA1 was present (without EBNA1, $p = 0.005$; with EBNA1, $p < 0.0001$; Fig. 3f). The mean fluorescence intensity of the GFP⁺ cells was similar in all cases, indicating that neither FANCA nor EBNA1 is simply affecting GFP expression (data not shown). These results indicate that FANCA strongly enhances ICL-induced HDR that is specifically coupled to replication.

To rule out possible effects from the TFO which remained joined to the ICL, we also performed assays in which the TFO was removed prior to transfection by using a pso-S-S-TFO for triplex formation, such that the disulfide bond between the ICL and the TFO was cleavable²⁶ (Supplementary Fig. 4). The ICL uncoupled from the TFO also induced HDR in U2OS cells in a replication-dependent manner ($p = 0.0002$; Fig. 3e). Importantly, ICL induction of HDR was again dependent upon the FA pathway component FANCA. ($p < 0.0001$; Fig. 3i), confirming that ICL-induced HDR repair in the TR-OriP-GFP reporter is substantially enhanced by both replication and the FA pathway.

The FA pathway has been linked to HDR since the discovery of the S-phase interaction of FANCD2 with BRCA1 and Rad51^{27,28}, although, curiously, FA core complex and FANCD2 have only mild HDR defects⁵. Here, we demonstrate a requirement for the FA pathway specifically in ICL-induced HDR coupled to replication. Defects in replication-coupled HDR are consistent with the hallmark of FA cells, namely ICL-induced chromosome aberrations¹. Because it would lead to unwinding of DNA adjacent to the ICL, replication may promote the incision step by providing a substrate for structure-specific nucleases (Fig. 3j). Whether repair typically occurs during collision of replication forks on both sides of the ICL³ (Fig. 3j) or just one side is as yet unclear. However, given that EBNA1 promotes unidirectional replication from OriP²⁹, collision of replication forks may not be necessary to promote repair. Direct assays for ICL-induced HDR *in vivo* and demonstration of the involvement of the FA pathway will facilitate the delineation of mechanisms and factors involved in this process.

Supplementary Material

Refer to Web version on PubMed Central for supplementary material.

Acknowledgments

We thank Katharina Schlacher, Jan LaRocque and Liz Kass from the Jasin lab for comments on the manuscript. This work was supported by MFAG grant 4765 from Associazione Italiana per la Ricerca sul Cancro (M.B.), the Hecksher Foundation for Children (M.E.M.), the Byrne Fund (M.J.), and National Institutes for Health grants P01CA94060 (M.E.M and M.J.) and R01GM54668 (M.J.).

Methods

Plasmids and cell lines

Plasmids phprtDRGFP (designated here as DR-GFP), pCBASce and pCAGGS vectors were previously described¹⁸. Plasmid phprtTRGFP (designated as TR-GFP) was generated as follows: PCR was performed with phprtDRGFP as a template using primers A to D, in which primers A and D flank SceGFP and primers B and C contain the TFO binding site, using Pfu Ultra (Stratagene). PCR was performed with primers A (5' AGTTGCTGAGCACGGCCCGGCTT) and B (5' GTCCCTCTCTCCTCTTTTCTTTTAAACTAGCCGGACACGCTGAACT) and in a separate reaction C (5' TTTAAAAGAAAAGAGGAGAAGAGGACACCTACGGCAAGCTGACCCTGAA) and D (5' TGATGCTATTGCTTTATTTGTAA), and then the products of the two reactions were combined for another round of PCR using primers A and D. The final 2-kb PCR product was cloned into the phprtDRGFP and pDRGFPhygro⁵ plasmid backbones cleaved with SgrAI and EcoRV giving rise to phprtTRGFP and pTRGFPhygro, respectively. To construct DR-OriP-GFP and TR-OriP-GFP, pDRGFPhygro and pTRGFPhygro were cleaved by Tth111I at two sites within the hygromycin resistance gene, dropping out a 1.5-kb fragment, and inserting a 2-kb OriP fragment from pCEP4 (Invitrogen, CA, USA), by amplifying OriP with primers oriPThiiiI-F (5' ATCGGACGGTGTCAACAACATTGCCTTTATGTGTAA) and oriPThiiiI-R (5' ATCGGACGGTGTCCAACCAGCAGGAAAAGGACAA), which flank the OriP sequence and contain TthIII sites.

Brca2 mutant hamster cells and chromosome-complemented cells were previously described¹⁶. Mutant mouse ES cell lines are referenced in the legend to Supplementary Table 1. For ICL assays with OriP plasmids, U2OS, GM6914 (FA-A) empty vector control, and GM6914 complemented with FANCA were stably transfected with pCEP4, with continuous selection in 0.3 $\mu\text{g ml}^{-1}$ hygromycin B and 1 $\mu\text{g ml}^{-1}$ puromycin.

Triplex formation and HDR assays

Pso-TFO, pso-mTFO, TFO, and pso-SS-TFO were synthesized by Eurogentec, Inc. (Seraing, Belgium). For triplex formation, 10 μM TFO (pso-TFO, TFO, or pso-mTFO) and 20 μg plasmid (TR-GFP or TR-OriP-GFP) were incubated together for 30 min in 40 μl 1X TFO buffer (1X TFO buffer: 50 mM HEPES, pH 7.2, 50 mM NaCl, 0.5 mM spermine, 10 mM MgCl_2).

For assays in which the ICL was formed *in vivo*, 40 μl triplex DNA was electroporated into 5×10^6 cells by pulsing at 250 V, 950 μF and then placed in a 10 cm tissue culture plate. After incubation for 1 hr at 37°C, the media was replaced with 1 ml PBS and then cells were irradiated with UVA (0.15 J cm^{-2} at 365 nm) using a Stratalinker (Stratagene, USA) with the lid removed. For the comparable DSB assays, 20 μg DR-GFP plasmid and 20 μg pCBASce or pCAGGS were cotransfected using the same electroporation conditions.

For assays in which the ICL was formed *in vitro*, 20 μl triplex DNA was irradiated with UVA (0.20 J cm^{-2} at 365 nm) using a Stratalinker (Stratagene, USA) with the test-tube lid open. To remove the TFO or non-crosslinked pso-TFO, 10 μg DNA was incubated with 50 μM complementary oligonucleotide in 1X TFO buffer at 70°C in 20 μl total volume for 10 min. For transfection, 2×10^5 cells were seeded into each well of a 6-well plate and incubated overnight at 37°C, and then 2 μg DNA per well was transfected using FuGENE6 transfection reagent (Roche) according to the manufacturer's instructions. For the comparable DSB assays, 0.4 μg DR-GFP or DR-OriP-GFP and 1.5 μg pCBASce were cotransfected using FuGENE6.

To form the ICL *in vitro* without a residual TFO tail, 2 μM pso-SS-TFO and TR-GFP or TR-OriP-TFO were incubated in TFO buffer. The ICL was formed by irradiating with UVA at 365 nm, and subsequently the DNA was incubated with 10 μM complementary oligonucleotide, followed by filtration through a TE-100 column (Clontech), to remove non-covalently associated pso-SS-TFO. To cleave the disulfide bond and separate the TFO from the ICL, DTT (0.1 M) treatment was performed in 10 mM Tris-HCl pH 8 and filtration was used to eliminate the remaining TFO. For transfection, 5×10^4 cells were seeded into each well of 24-well plate. After overnight incubation at 37°C, 0.4 μg of ICL:TR-GFP or ICL:TR-OriP-GFP plasmid were transfected into each well with FuGENE6.

To determine the amount of ICL or DSB-induced HDR, the percentage of cells that were GFP⁺ was quantitated by flow cytometric analysis 48 hrs after transfection with a Becton Dickinson FACScan. In human cells, a cotransfected DsRed expression vector (2.4 μg) was used to monitor transfection efficiency. U2OS cells typically transfected 2 to 3 times better than complemented or uncomplemented GM6914 cells. All human data were analyzed with an unpaired *t* test; mouse ES cell data were analyzed with a paired *t* test (Supplementary Table 1).

DraI protection assay

For DNA in which the crosslink was formed *in vivo*, the DraI protection assay was performed as described¹¹. DNA was extracted from cells with the QIAamp DNA blood mini kit (QIAGEN, Venlo, Netherlands). To remove TFO or non-crosslinked pso-TFO from TR-GFP, 1 μg of the extracted DNA was incubated with 20 μM complementary oligonucleotide in 1X TFO buffer at 70°C in 20 μl total volume for 10 min, and then cooled to room temperature at 10°C min^{-1} . For DraI digestion, 2.5 μl 10X DraI buffer plus 5 U DraI (Roche) (total volume of 5 μl) was added and incubated for 3 hr at 37°C. DNA fragments were analyzed by Southern blotting using a GFP fragment as probe.

References

1. Auerbach AD. *Mutat Res.* 2009; 668:4–10. [PubMed: 19622403]
2. Wang W. *Nat Rev Genet.* 2007; 8:735–748. [PubMed: 17768402]
3. Raschle M, et al. *Cell.* 2008; 134:969–980. [PubMed: 18805090]
4. Knipscheer P, et al. *Science.* 2009; 326:1698–1701. [PubMed: 19965384]
5. Nakanishi K, et al. *Proc Natl Acad Sci USA.* 2005; 102:1110–1115. [PubMed: 15650050]
6. Moynahan ME, Jasin M. *Nat Rev Mol Cell Biol.* 2010; 11:196–207. [PubMed: 20177395]
7. Pierce AJ, Johnson RD, Thompson LH, Jasin M. *Genes Dev.* 1999; 13:2633–2638. [PubMed: 10541549]
8. Faruqi AF, Seidman MM, Segal DJ, Carroll D, Glazer PM. *Mol Cell Biol.* 1996; 16:6820–6828. [PubMed: 8943337]
9. Chin JY, Glazer PM. *Mol Carcinog.* 2009; 48:389–399. [PubMed: 19072762]
10. Vasquez KM. *Environ Mol Mutagen.* 2010; 51:527–539. [PubMed: 20196133]
11. Brunet E, Corgnali M, Cannata F, Perrouault L, Giovannangeli C. *Nucleic Acids Res.* 2006; 34:4546–4553. [PubMed: 16951289]
12. Giovannangeli C, Thuong NT, Helene C. *Nucleic Acids Res.* 1992; 20:4275–4281. [PubMed: 1508719]
13. Kalish JM, Seidman MM, Weeks DL, Glazer PM. *Nucleic Acids Res.* 2005; 33:3492–3502. [PubMed: 15961731]
14. Liu Y, Nairn RS, Vasquez KM. *Nucleic Acids Res.* 2008; 36:4680–4688. [PubMed: 18628293]
15. Zhang N, Liu X, Li L, Legerski R. *DNA Repair (Amst).* 2007; 6:1670–1678. [PubMed: 17669695]
16. Kraakman-van der Zwet M, et al. *Mol Cell Biol.* 2002; 22:669–679. [PubMed: 11756561]
17. Saeki H, et al. *Proc Natl Acad Sci USA.* 2006; 103:8768–8773. [PubMed: 16731627]
18. Pierce AJ, Hu P, Han M, Ellis N, Jasin M. *Genes Dev.* 2001; 15:3237–3242. [PubMed: 11751629]
19. Kass EM, Jasin M. *FEBS Lett.* 2010; 584:3703–3708. [PubMed: 20691183]
20. Adamo A, et al. *Mol Cell.* 2010; 39:25–35. [PubMed: 20598602]
21. Pace P, et al. *Science.* 2010; 329:219–223. [PubMed: 20538911]
22. Hinz JM. *Environ Mol Mutagen.* 2010; 51:582–603. [PubMed: 20658649]
23. Stark JM, Pierce AJ, Oh J, Pastink A, Jasin M. *Mol Cell Biol.* 2004; 24:9305–9316. [PubMed: 15485900]
24. D'Andrea AD, Grompe M. *Nat Rev Cancer.* 2003; 3:23–34. [PubMed: 12509764]
25. Reisman D, Yates J, Sugden B. *Mol Cell Biol.* 1985; 5:1822–1832. [PubMed: 3018528]
26. Guillonneau F, Guieysse AL, Nocentini S, Giovannangeli C, Praseuth D. *Nucleic Acids Res.* 2004; 32:1143–1153. [PubMed: 14966263]
27. Garcia-Higuera I, et al. *Mol Cell.* 2001; 7:249–262. [PubMed: 11239454]
28. Taniguchi T, et al. *Blood.* 2002; 100:2414–2420. [PubMed: 12239151]
29. Lindner SE, Sugden B. *Plasmid.* 2007; 58:1–12. [PubMed: 17350094]
30. Havre PA, Gunther EJ, Gasparro FP, Glazer PM. *Proc Natl Acad Sci USA.* 1993; 90:7879–7883. [PubMed: 8356097]

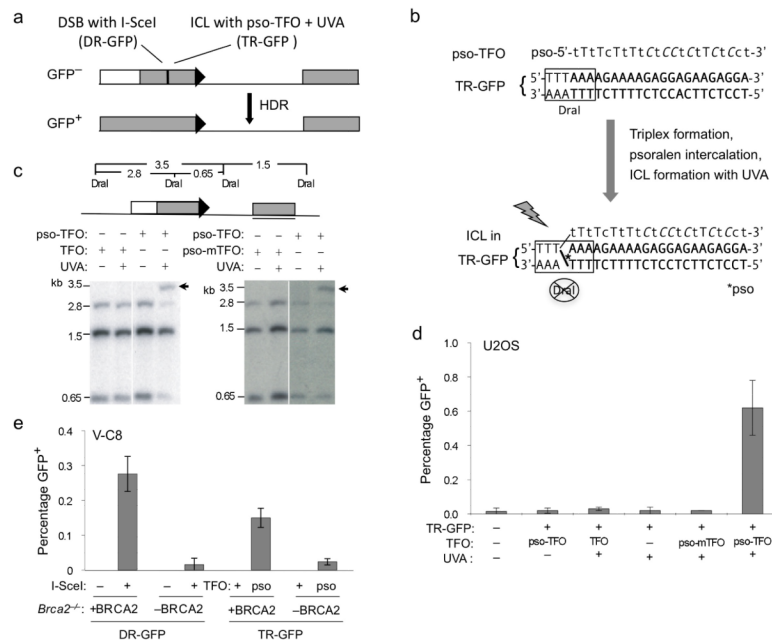


Figure 1. ICL induction of HDR in mammalian cells

(a) HDR reporters. After DNA damage in the upstream *GFP* repeat, HDR with the downstream *GFP* repeat leads to a *GFP*⁺ gene. A site-specific ICL forms from psoralen conjugated to a TFO (pso-TFO)³⁰. A site-specific DSB is formed by I-SceI endonuclease. (b) ICL formation in TR-GFP. The TFO binds to the TR-GFP plasmid sequence forming a triplex. Psoralen intercalates at the TpA site, which after UVA exposure forms an ICL, blocking DraI cleavage. Lower case nucleotides within the TFO are locked nucleic acids (LNA) which enhance the stability of the triplex *in vivo*¹¹; all cytosines are methylated at position 5. (c) DraI protection assay to quantify *in vivo* ICL formation. DNA was isolated from U2OS cells transfected with pso-TFO:TR-GFP and treated with UVA. Unconjugated TFO was the control in the left panel and a conjugated TFO which cannot bind TR-GFP (pso-mTFO) was the control in the right panel. ICL formation is distinguished from non-covalent triplex DNA formation by addition of an oligonucleotide complementary to the TFO prior to DraI cleavage which binds to the TFO released from the triplex upon heating (Supplementary Fig. 1d). The 3.5-kb fragment is indicative of ICL formation (arrow). Thin bar, probe. (d) ICL-induced HDR in U2OS cells. Triplexes formed *in vitro* were transfected into U2OS cells which were then treated with UVA. *GFP*⁺ cells arise from HDR of the ICL in TR-GFP, and are significantly lower without UVA or pso-TFO ($p=0.0003$, unpaired *t* test). Transfection efficiency is monitored by cotransfection of a DsRed expression vector. Error bars, ± 1 SD; $n=4$ replicates from 2 independent experiments. (e) ICL-induced HDR, like DSB-induced HDR, is significantly reduced in *Brca2* mutant V-C8 cells compared with BRCA2-complemented V-C8 cells ($p<0.0001$). Triplexes formed between TR-GFP and either pso-TFO (pso) or an unmodified TFO (+) were transfected into cells which were then treated with UVA. For DSB-induced HDR, DR-GFP was transfected into cells with or without the I-SceI expression vector. $n=5$ replicates from 2 independent experiments.

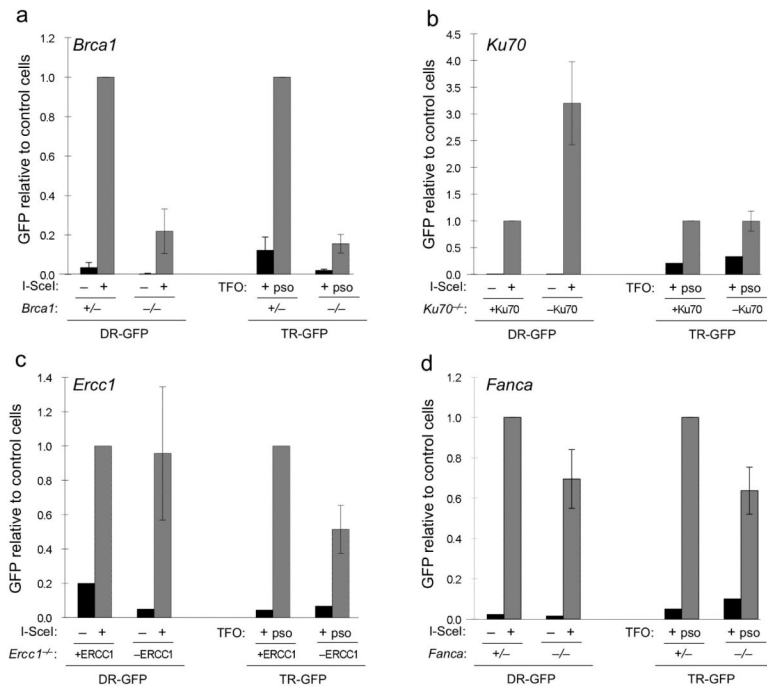


Figure 2. ICL and DSB-induced HDR in mouse ES cell mutants

Percentage GFP⁺ cells for each mutant was normalized to the indicated control. BRCA1-deficient cells have substantially reduced ICL and DSB-induced HDR (a); Ku70-deficient cells only have increased DSB-induced HDR (b); ERCC1-deficient cells only have reduced ICL-induced HDR (c); FANCA-deficient cells have mildly reduced ICL and DSB-induced HDR (d). For ICL-induced HDR, cells were transfected with pso-TFO:TR-GFP or TFO:TR-GFP and then treated with UVA. Error bars, ± 1 SD. See Supplementary Table 1 for statistical analysis.

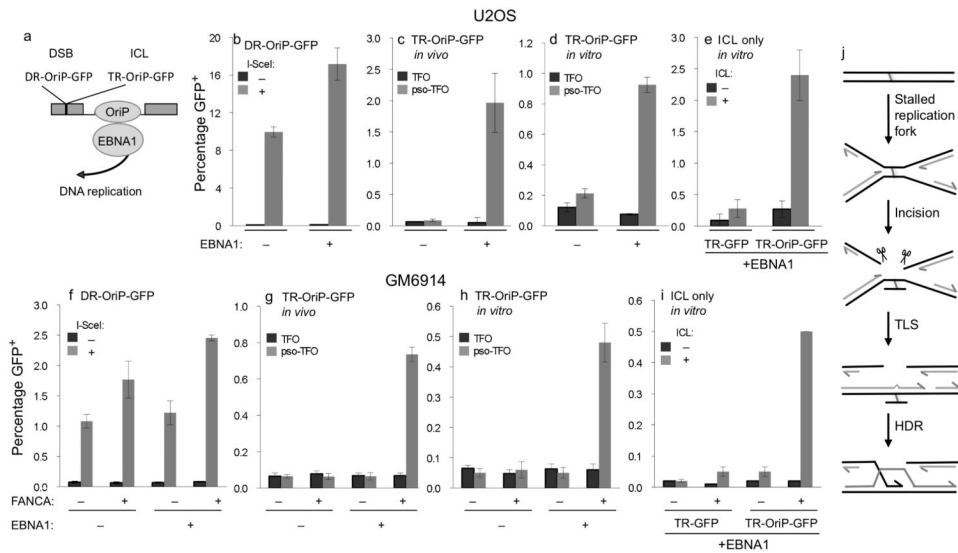


Figure 3. FANCA-dependent, replication-coupled ICL-induced HDR

(a) HDR reporters with EBV OriP for replication in EBNA1-expressing cells. (b-e) HDR assays in U2OS cells stably expressing EBNA1 (+) or not (-). DSB-induced HDR is only moderately increased with EBNA1/OriP (b), whereas ICL-induced HDR is substantially increased with EBNA1/OriP from either *in vivo* (c) or *in vitro* ICL formation without (d) or with (e) removal of the TFO tail. All comparisons of I-SceI or pso-TFO plus or minus EBNA1/OriP have $p \leq 0.0002$. Error bars, ± 1 SD; $n=4$ or 5 replicates from 2 independent experiments. (f-i). HDR assays in GM6914 or FANCA-complemented GM6914 cells expressing EBNA1 (+) or not (-). DSB-induced HDR is moderately increased with FANCA and EBNA1/OriP (f). With EBNA1, \pm FANCA $p=0.0001$; without EBNA1, \pm FANCA $p=0.005$; with FANCA, \pm EBNA1 $p=0.004$; without FANCA, \pm EBNA1 $p=0.26$. $n=4$ replicates from 2 independent experiments. By contrast, ICL-induced HDR is substantially increased with FANCA and EBNA1/OriP from either *in vivo* (g) or *in vitro* ICL formation without (h) or with (i) removal of the TFO tail. With EBNA1 and FANCA, $p < 0.0001$ compared with any other condition. Error bars, ± 1 SD; $n=4$ to 6 replicates from 2 or 3 independent experiments (g,h); $n=3$ replicates from 1 experiment (i). For *in vivo* ICL formation, TR-OriP-GFP bound to the indicated triplex was transfected into cells which were then treated with UVA. For *in vitro* TFO formation, TR-OriP-GFP was bound to the indicated triplex and then exposed to UVA prior to transfection. j. Model for ICL repair by HDR. ICLs stall converging replication forks. Incisions on both sides of the ICL create strand breaks, and translesion synthesis (TLS) allows replication past the lesion. The adduct is removed and strand invasion leads to HDR. As replication from OriP has been reported to be predominately unidirectional²⁹, HDR in TR-GFP likely proceeds after stalling of a single replication fork.